4

Effect of flubendiamide in the CAM Angiogenesis of developing chick embryo

INTRODUCTION

According to Troczka et al. (2017), the phthalic acid diamide flubendiamide has been approved for use on more than two hundred different types of crops, including soybeans, almonds, tobacco, peanuts, cotton, lettuce, tomatoes, melons and bell peppers. The primary objective behind the introduction of flubendiamide was to suppress the population of caterpillars of lepidopteran pests. Nauen & Steinbach (2016) state that it primarily targets calcium release channels, resulting in paralysis in the muscular fibers of the stomach. This ultimately leads to the cessation of feeding by the larvae, eventually resulting in death due to starvation. Recent research has raised concerns about the effects of flubendiamide on non-target organisms, such as the fruit fly (*Drosophila melanogaster*) and the Chinese tiger frog (*Hoplobatrachus chinensis*) (Li et al., 2014).

In 2016, the Environmental Protection Agency of the United States came to the conclusion that continuous use of flubendiamide will lead to unreasonably negative impacts on the environment, including the biotic component of the substance (Sun et al., 2018). Research by Sarkar et al. (2014, 2017 and 2018) has demonstrated that flubendiamide is neurotoxic and can cause structural abnormalities in *D. melanogaster*. Additionally, Liu et al. (2022) reported the presence of flubendiamide residues in human milk, raising concerns about the potential health risks for both mothers and their infants. Consequently, conducting a safety assessment of flubendiamide is crucial to evaluate its potential developmental toxicity in children.

Because of the molecular, cellular and anatomical similarities that exist between the human embryo and the chick embryo, the chick embryo was selected for the purpose of this inquiry. Because of the resemblance, the chick embryo is a very helpful instrument to obtain an understanding of the activities that take place during the development process (Stern, 2018). The ease of maintenance and the ability to grow outside of the uterus, which helps to spare the mother's life, were two additional features that were regarded as being beneficial (Stern, 2018).

A preliminary investigation conducted in the lab revealed major developmental abnormalities in the growing chick embryo. Based on these findings, we hypothesized that flubendiamide inhibits angiogenesis in the chick chorioallantoic membrane (CAM). Angiogenesis, a pivotal process in development, involves the formation of new blood vessels. According to Felmeden et al. (2003) and Wittig and Munsterberg (2016) the intricate network of blood vessels that is generated through angiogenesis plays a crucial part in the process of giving oxygen and nutrients to developing tissues during the embryonic stage. This helps to ensure that the tissues are able to grow and develop in the appropriate manner.

According to Felmeden et al. (2003), this network is responsible for supporting numerous processes, including development, repair and homeostasis, which contribute to the general balance and stability of tissues. The CAM of the chick, which is an extraembryonic tissue, is an example of this vascularized system. During the process of embryonic development, the CAM plays a significant role in facilitating gas exchange, nutrition transfer and waste disposal for the growing chick embryo (Figure 4.1). This highlights the necessity of angiogenesis in maintaining the proper functioning of important physiological processes (Ahmed et al., 2022).

The process of CAM angiogenesis begins in the developing chick embryo with the development of blood islands on day 2 and then continues with the emergence of primitive blood vessels and further vascularization on day 3. It is important to note that on day 4, the allantoic epithelium makes a significant contribution to the creation of the bilayered CAM (Schmidt et al., 2019). Following this, there is a time period during which the primitive blood vessels undergo a phase of expansion and branching from day 6 to day 9, followed by the maturity of the vascular network from day 10 to day 14.

On days 15 to 18, the vascular density inside the CAM rises, supporting accelerated gas exchange and nutrition transfer (Schmidt et al., 2019). This occurs as embryonic development progresses. In the end, the vascular system within the CAM reaches its final condition between days 19 and 21, providing essential support for the developing embryo. This brings the dynamic process of CAM angiogenesis to a successful conclusion throughout the 21-day incubation period (Schmidt et al., 2019).

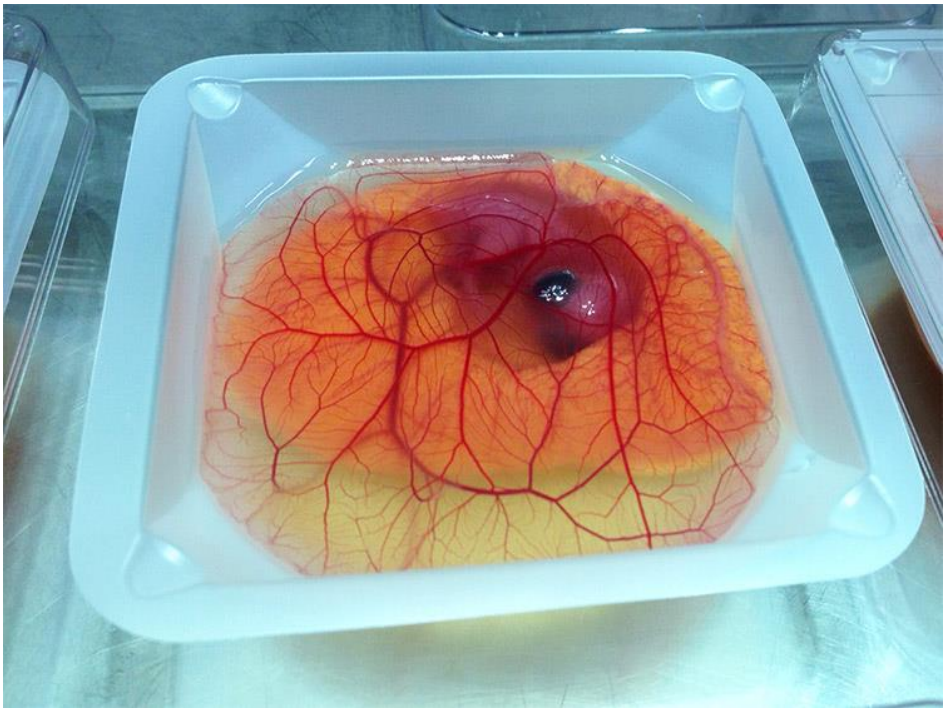

Figure 4.1: Chick chorioallantoic membrane in shell-less culture (https://www.kmlvision.com/wp-content/uploads/2022/01/2021-kmlvision-interview-angiogenesis-Figure-1-web.jpg)

During the process of embryonic development, blood vessels serve as a conduit for the delivery of oxygen and nutrients, which in turn maintain cellular metabolism and the creation of energy. While this is happening, blood vessels are responsible for facilitating the clearance of waste products that are produced by developing cells. This helps to ensure that the environment is favorable for the creation of healthy cells. Although there are many elements that contribute to the creation of blood vessels, VEGF plays an important role in this process. Angiogenesis is a dynamic process that involves the development of new blood vessels and the initiation of a cascade of molecular processes (Hiratsuka et al., 2005). VEGF and its receptor KDR (VEGFR-2) play a critical role in orchestrating angiogenesis. Research by Pulkkinen et al. (2021) demonstrated that VEGF stimulates angiogenesis by activating BMP2 and BMP6. Additionally, studies by Karar and Maity (2011) and Guo et al. (2018) found that VEGF is a powerful activator of various downstream pathways, including the PI3K-Akt/mTORC2 pathway, which are essential for angiogenesis. Therefore, an effort was made to unravel the molecular processes that are responsible for the reduction in chicken chorioallantoic membrane angiogenesis that was caused by flubendiamide.

MATERIALS AND METHODS

The objective of this study was to assess the impact of flubendiamide on angiogenesis in the chorioallantoic membrane of developing chick embryos. Eggs were randomly assigned to experimental groups, with embryos collected on days 2, 3 and 4 for analysis. Each experiment included three repetitions, with thirty eggs per group.

Following a dosage range examination, LD_{50} of flubendiamide was determined. The concentration of 500 ppm was identified as the LOEC. In subsequent trials, the treatment group received flubendiamide at 500 ppm, while the control group received 50 µl of PBS.

AngioTool 0.6 software was used to analyze the morphological and geographical parameters of the vascular networks within the CAM of day 3 and day 4 embryos. The parameters assessed included lacunarity, total vessel length, vessel density and the number of vessel junctions.

For molecular studies, Auto Dock Tools 4.2.2 software predicted the binding energies of flubendiamide with proteins involved in the apoptotic pathway and CAM angiogenesis. Protein structures were sourced from the PDB and converted into PDB files using BIOVIA Discovery Studio Visualizer version 21.1.0.20298.

qRT-PCR and Western blot techniques were used to investigate the levels of transcripts and proteins associated with CAM angiogenesis.

Immunohistochemistry was conducted to evaluate the expression of Cl. Caspase-3 in both control and treated embryos. Data analysis was carried out using GraphPad Prism 8.0, with results presented in graphical form.

Statistical analysis was performed using Student's t-test, maintaining a 95% significance level.

RESULTS

Analysis of the CAM vasculature

In order to study vascular networks of CAM in 3- and 4-day embryos, vessel density number, vascular junctions, length and lacunarity were analyzed. Compared to control embryos of days 3 and 4, fewer vessels were present in treatment groups ($p \leq 0.001$). The vessel density and number of vessel junctions were also reduced in treated embryos. The total length of the vessel showed a marginal reduction on both days in treated embryos. The lacunarity measures the empty spaces in the spatial distribution in the CAM images. High lacunarity (empty spaces between blood vessels) values can be seen in treated groups contrastingly with control ($p \leq 0.001$) (Figure 4.2). Analysis of the day 3 and 4 embryos corroborates the results of the AngioTool analysis. Vessel density decreased drastically in the treated groups compared to the control ($p \leq 0.001$) (Table 4.1). The total vessel length and junctions also reduced significantly ($p \leq 0.001$). The mean lacunarity is high in treated groups, validating empty space in the treatment due to the absence of vessels (Figure 4.3).

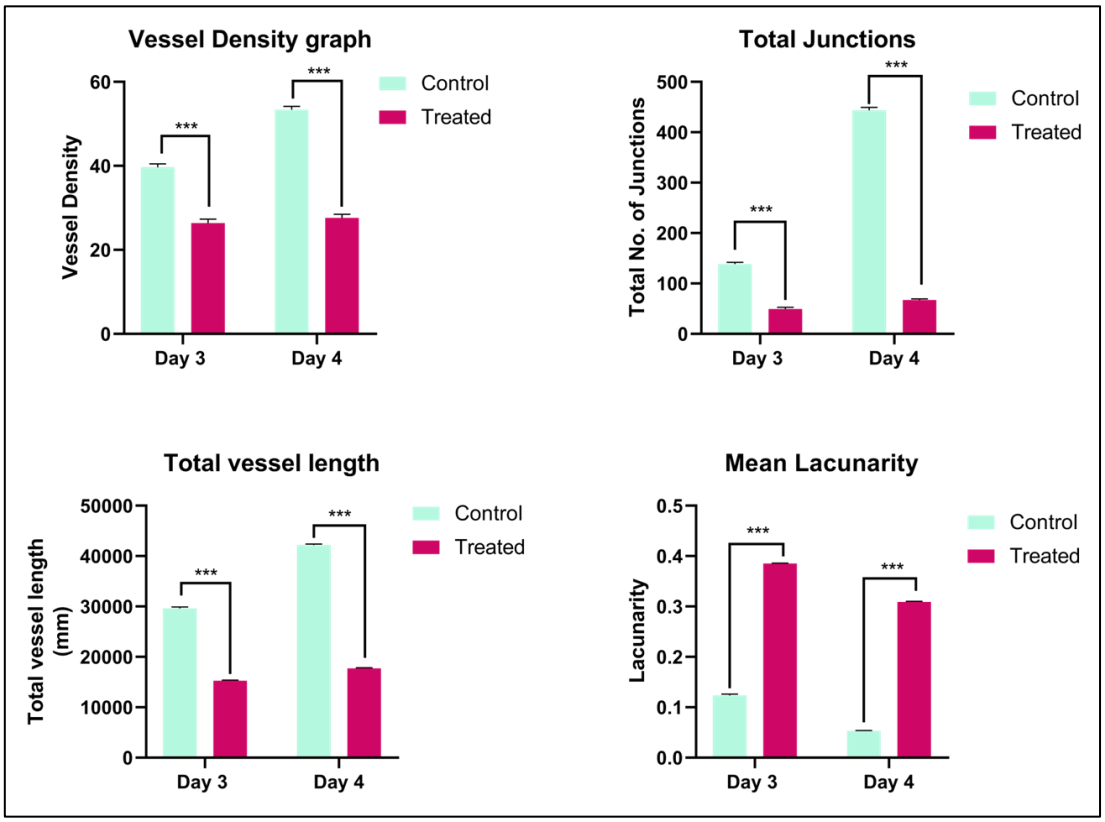

Figure 4.2: Analysis of CAM angiogenesis in flubendiamide-treated day 3 and 4 embryos. n=6; ***p≤0.001.

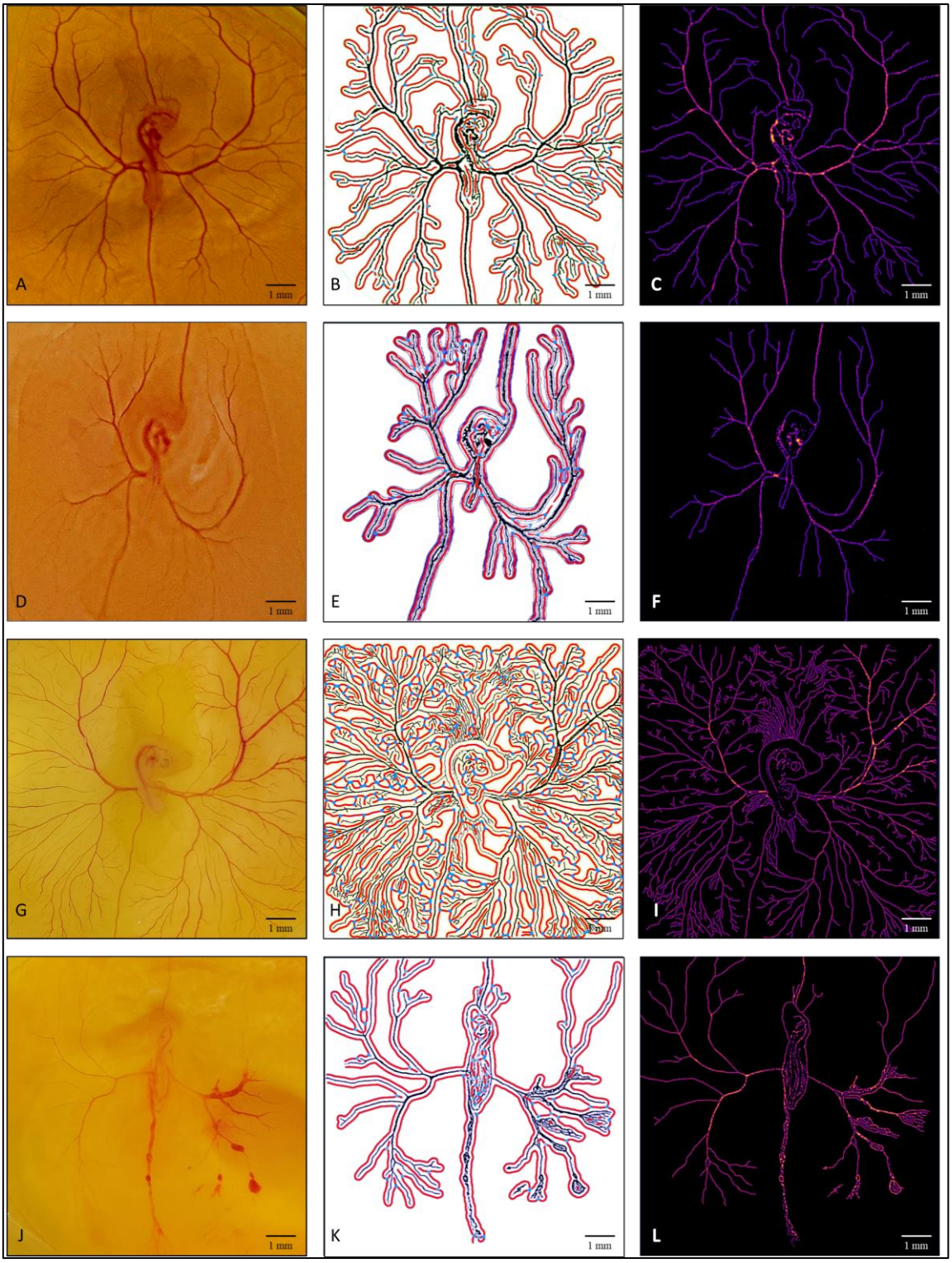

Figure 4.3: Detection of vascular network architecture: **A, B, C**: Day 3 control embryo; **D, E, F**: Day 3 treated embryo; **G, H, I**: Day 4 control embryo; **J, K, L**: Day 4 treated embryo. Column 1: CAM images of the chick embryos Control and Treated; Column 2: Architectural layout of the vascular network (red lines) processed on AngioTool software, illustrating the junctions denoting vessel bifurcations (blue dots); Column 3: Skeletal image viewed on Fiji software.

Molecular docking for CAM angiogenesis and apoptosis target protein

Flubendiamide subjected to docking analyses with key proteins associated with the CAM angiogenic and apoptotic pathways exhibited favorable docking scores: VEGFα (6MXR) at the active site with a docking score of -8.3 kcal/mol, WNT7A with a score of -8.7 kcal/mol, followed by PI3K (1YI3) with -7.4 kcal/mol, BMP2 (2GOO) with -7.3 kcal/mol and CASPASE-3 (4QTX) with -7.2 kcal/mol (Figure 4.4). The docking process also revealed the formation of different types of bonds between flubendiamide and the mentioned proteins (Table 4.2). The high binding affinity observed implies that flubendiamide may influence the functionality of these proteins, potentially contributing to the reduction of blood vessel development in CAM angiogenesis in treated embryos compared to the control.

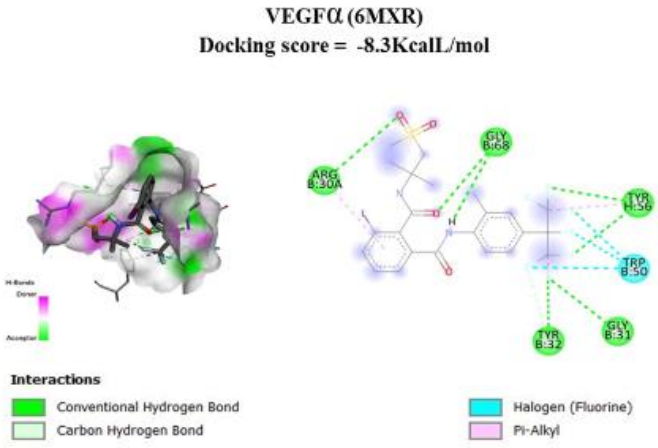

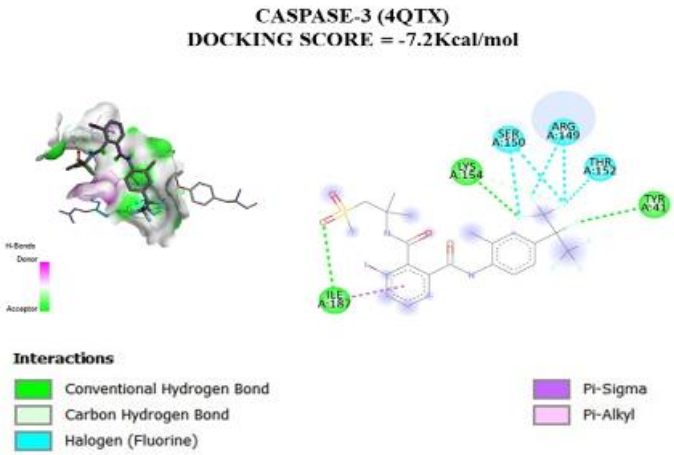

BMP2 (2GOO)
DOCKING SCORE = -7.3Kcal/mol

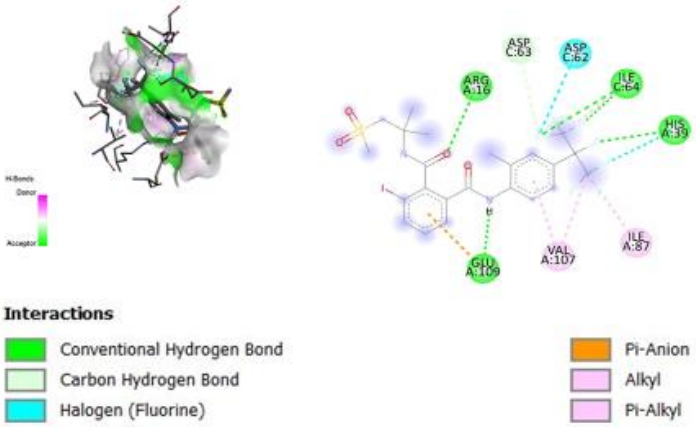

Interactions

- Conventional Hydrogen Bond
- Carbon Hydrogen Bond
- Halogen (Fluorine)
- Pi-Anion
- Alkyl
- Pi-Alkyl

PI3K (1YI3)
Docking score = -7.4Kcal/mol

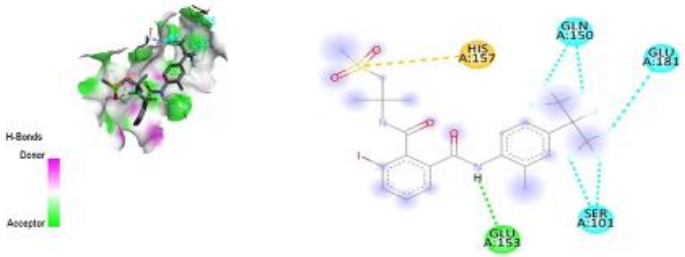

Interactions

- Conventional Hydrogen Bond
- Halogen (Fluorine)
- Pi-Sulfur

WNT7A (8TZO)
Docking score = -8.7Kcal/mol

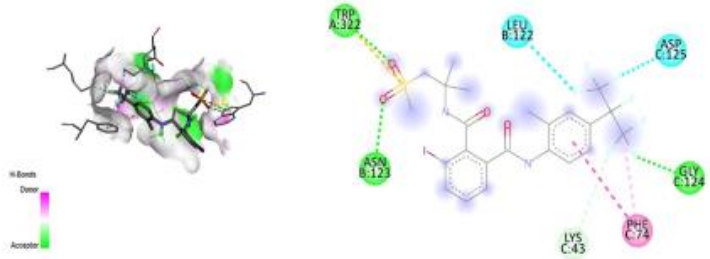

Interactions

- Conventional Hydrogen Bond
- Carbon Hydrogen Bond
- Halogen (Fluorine)
- Pi-Sulfur
- Pi-Pi Stacked
- Pi-Alkyl

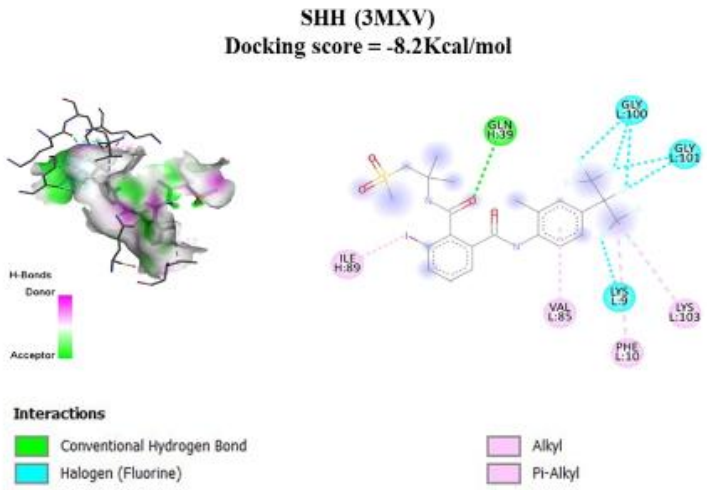

Figure 4.4: Molecular docking 3D and 2D structure of flubendiamide with VEGFα (6MXR), CASPASE-3 (4QTX), BMP2 (2GOO), PI3K (1YI3), WNT7A (8TZO) and SHH (3MVX)

Angiogenesis-related gene expression profile

The transcriptional status of SHH, VEGFα, CASPASE-3, KDR, WNT7A, BMP2, BMP6, AKT, PI3K, PCNA and RHOB were examined on days 2, 3 and 4 in the control and treated embryos. In day 2 embryos, the relative mRNA expression levels of CASPASE-3 were significantly higher ($p \leq 0.01$) in the treatment groups compared to the controls. PCNA was downregulated by more than one-fold compared to the control groups. VEGFα ($p \leq 0.01$), BMP2 ($p \leq 0.05$), AKT ($p \leq 0.05$) and PI3K ($p \leq 0.05$) were marginally reduced in the treated group. No significant changes were seen in SHH, KDR, RHOB, BMP6 and WNT7A. On day 3, CASPASE-3 ($p \leq 0.001$) was upregulated by five-fold and RHOB by two-fold compared to the control groups. VEGFα remained downregulated. No significant changes were seen in SHH, KDR, WNT7A, BMP2, or PI3K. BMP6 ($p \leq 0.05$), AKT ($p \leq 0.05$) and PCNA ($p \leq 0.05$) were marginally reduced in the treated group. The qRT-PCR analysis in day 4 embryos showed that SHH ($p \leq 0.05$), VEGFα ($p \leq 0.01$), KDR ($p \leq 0.05$), WNT7A ($p \leq 0.05$), BMP2 ($p \leq 0.001$), BMP6 ($p \leq 0.05$) and PI3K ($p \leq 0.05$) expressions were significantly downregulated. The change in expression levels of AKT was found to be statistically insignificant. PCNA and RHOB showed increased expression. CASPASE-3 remained high ($p \leq 0.01$) in the treated embryos (Figure 4.5; Table 4.3).

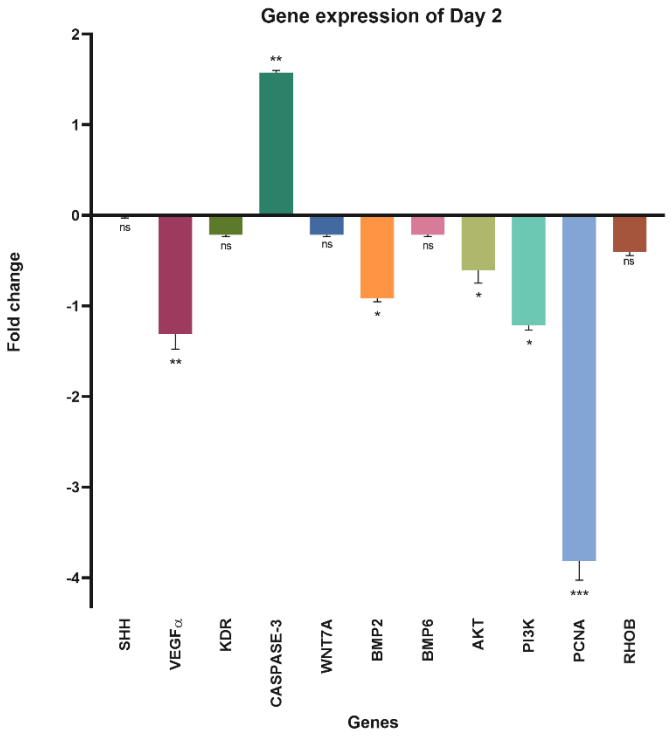
Gene expression of Day 2
Fold change
2
1
0
-1
-2
-3
-4
**
ns
**
ns
ns
*
ns
*
*
***
ns
SHH
VEGFα
KDR
CASPASE-3
WNT7A
BMP2
BMP6
AKT
PI3K
PCNA
RHOB
Genes

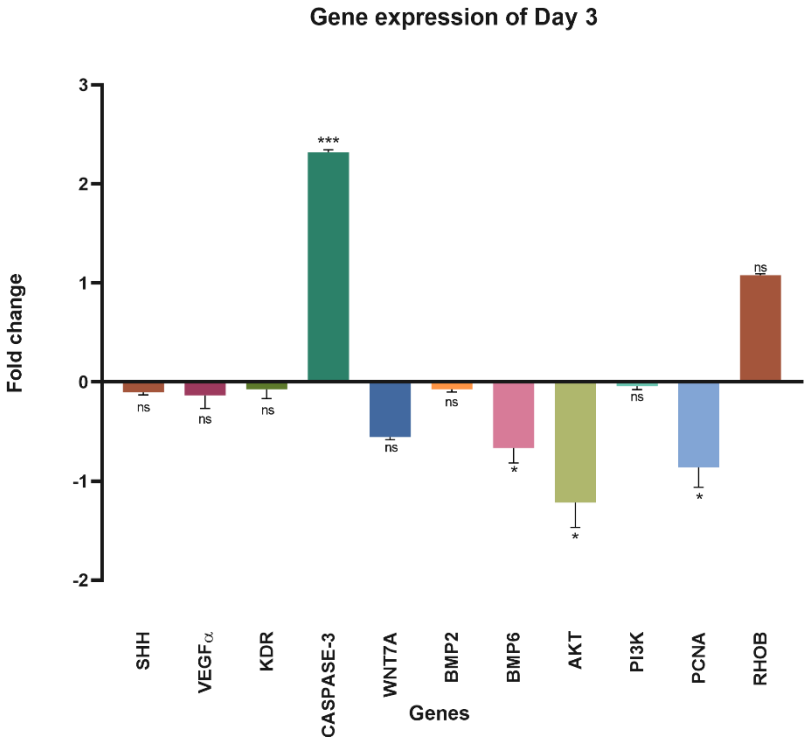
Gene expression of Day 3
Fold change
3
2
1
0
-1
-2
ns
ns
ns
***
ns
ns
*
*
ns
*
ns
SHH
VEGFα
KDR
CASPASE-3
WNT7A
BMP2
BMP6
AKT
PI3K
PCNA
RHOB
Genes

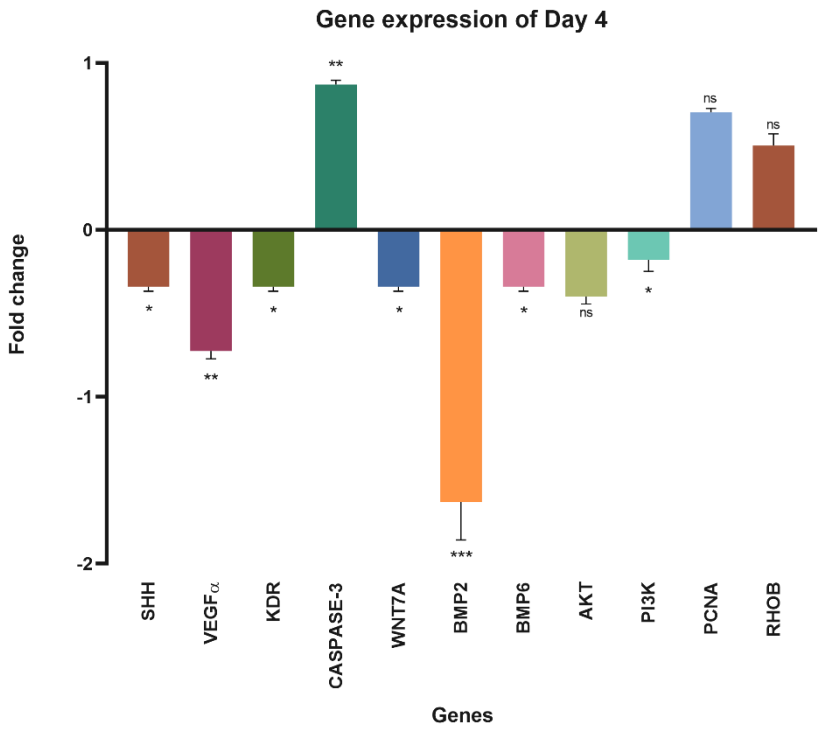

Figure 4.5: Transcript levels of genes regulating CAM angiogenesis in flubendiamide treated day 2, 3 and 4 embryos: Values are expressed in fold change (Mean ± SEM). Fold change values for the control embryo are 1.0 for all the genes. Graph in Log 10 of fold change; n=3 with 30 eggs per group per experiment. *p≤0.05; **p≤0.01; ***p≤0.001.

Angiogenesis-related protein expression profile

In order to confirm the results obtained from qRT-PCR, a western blot analysis was carried out to assess the protein expression levels of crucial regulators involved in CAM angiogenesis. The quantitative analysis of the bands consistently demonstrated decreased expression of Vegfα, Akt and Pi3k in treated embryos on days 2, 3 and 4 compared to the control group. More precisely, the expression of Vegfα was seen to be lower on days 2 ($p \leq 0.05$), 3 ($p \leq 0.01$) and 4 ($p \leq 0.01$) in the treatment group compared to the control group. Similarly, AKT and PI3K showed reductions on days 2 ($p \leq 0.01$), 3 ($p \leq 0.01$) and 4 ($p \leq 0.001$ and $p \leq 0.01$, respectively). Furthermore, the treated embryos exhibited a significant rise in Cl. Caspase-3 expression compared to the control group on days 2 ($p < 0.01$), 3 ($p \leq 0.001$) and 4 ($p \leq 0.05$). The findings corroborate the patterns revealed in the qRT-PCR results (Figure 4.6; Table 4.4). GAPDH was employed as an internal control to verify the precision and dependability of the protein expression analysis.

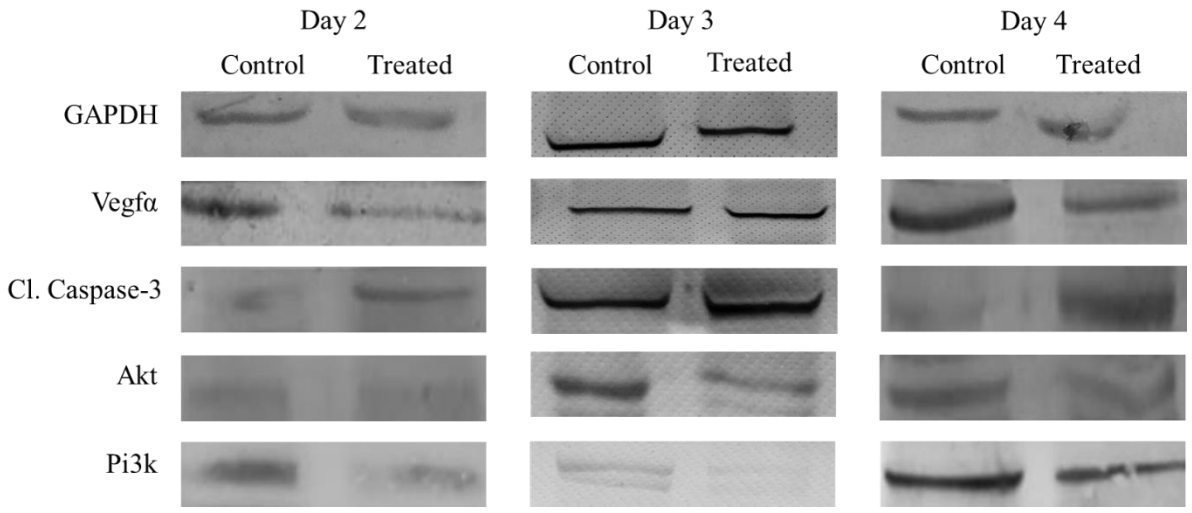
Day 2
Day 3
Day 4
Control
Treated
Control
Treated
Control
Treated
GAPDH
Vegfα
Cl. Caspase-3
Akt
Pi3k

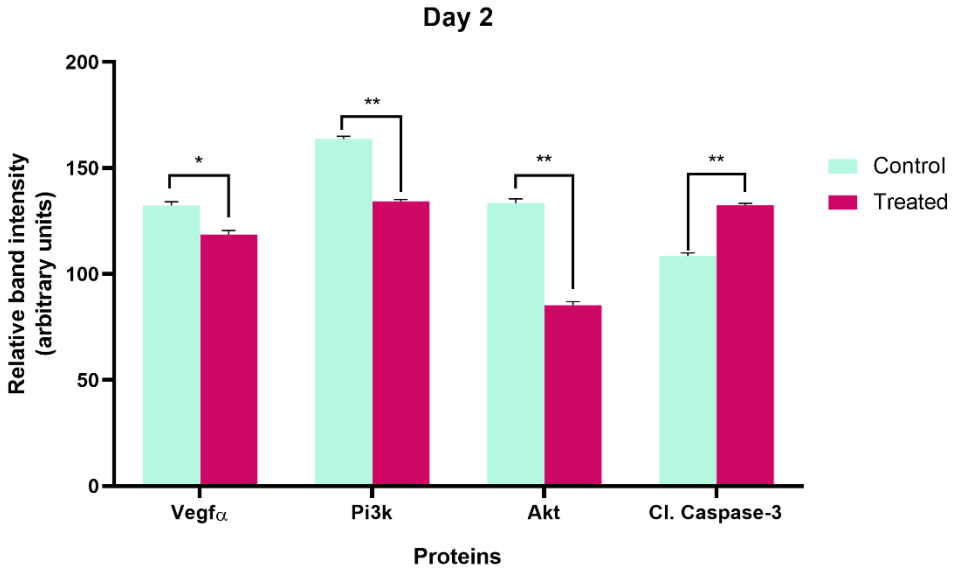
Day 2
Relative band intensity (arbitrary units)
200
150
100
50
0
*
**
**
**
Vegfα
Pi3k
Akt
Cl. Caspase-3
Proteins
Control
Treated

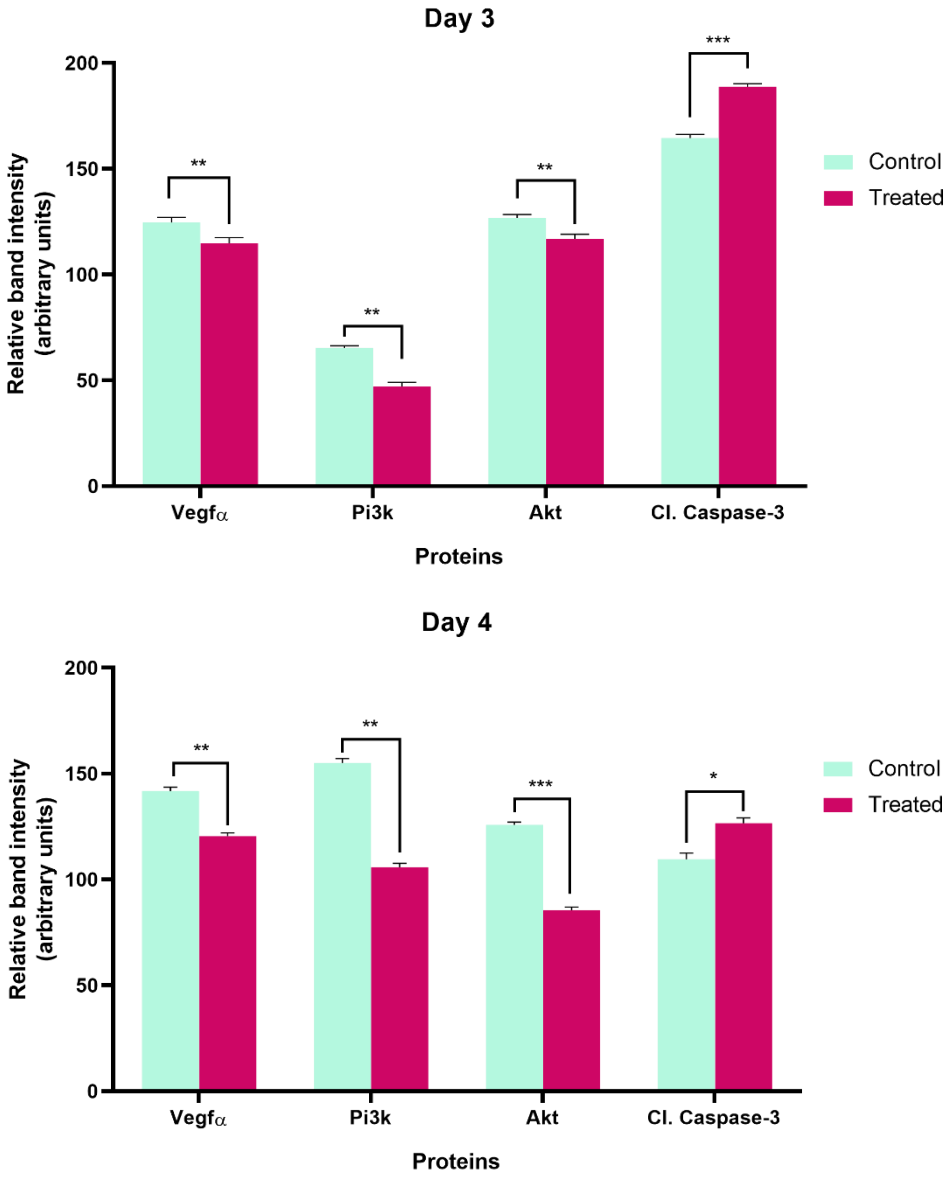

Figure 4.6: Western Blot images showing comparative expressions on days 2, 3 and 4. GAPDH was taken as loading control, n=3 with 30 eggs per group per day; *p≤0.05; **p≤0.01; ***p≤0.001.

Assessment of apoptosis by immunohistochemistry

Both qRT-PCR and Western blot tests revealed that the levels of Cl. Caspase-3 were elevated. To establish the location of apoptosis within the CAM, immunohistochemistry was performed on entire embryos after day 2 of development. Localization revealed that Cl. Caspase-3 was expressed along the primary vessels of the CAM. The vessels in the control group displayed well-formed structures without any visible blue dots. In contrast, the treated group exhibited a reduction in the number of blood vessels, with clear blue spots visible in the regions of the

vessels, indicating the presence of Cl. Caspase-3. According to these findings, the treated group had a significantly higher level of Cl. Caspase-3 compared to the control group (Figure 4.7).

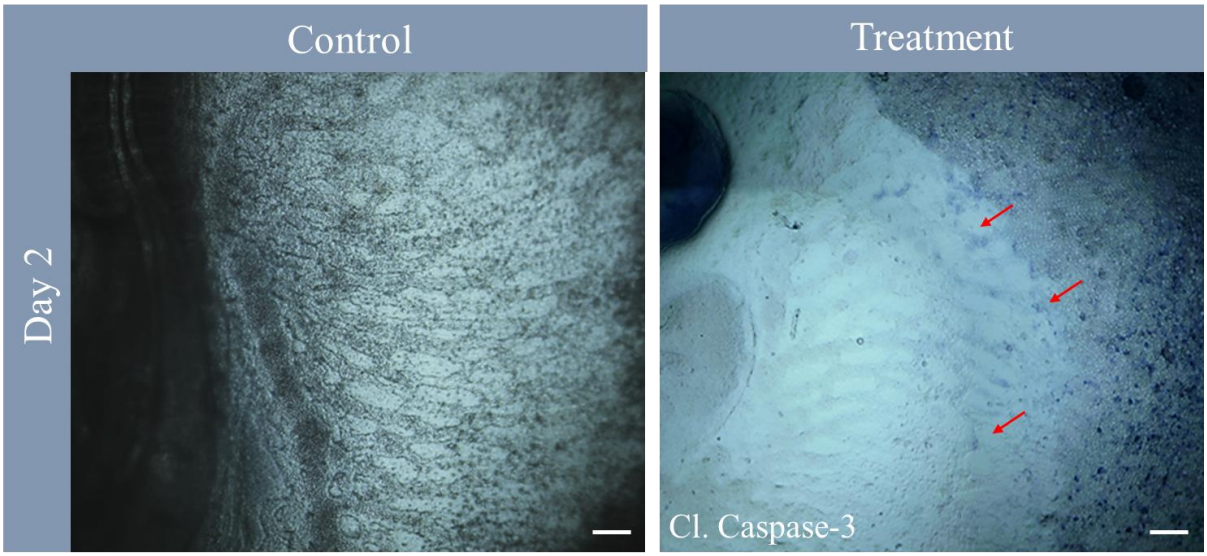

Figure 4.7: Imunohistochemical localization of Cl. Caspase-3 in a day 2 chick embryos. Blue-stained region indicates the presence of Cl. Caspase-3 (shown by red arrow). A negative control for the primary antibody is shown as a control. The scale bar represents 500 µm.

DISCUSSION

Pesticides, as defined by the Food and Agriculture Organization (FAO), are chemical substances used to control, prevent, or eliminate pests. These are commonly employed to improve crop yield by specifically targeting pests that disrupt crop growth, storage, or processing (WHO, 2016). The extensive use of pesticides has resulted in their enduring existence in the environment, inadvertently subjecting non-target creatures to their detrimental consequences. Scientific research has verified that when non-target organisms are exposed to pesticides, they may experience harmful reactions, such as congenital malformations (Kalliora et al., 2018). Nevertheless, the precise mechanisms responsible for these effects are still not fully understood. Research indicates that prolonged exposure to chlorfenvinphos, an organophosphate insecticide impairs blood vessel function in mammals (Xiao-Ming et al., 2010). Another study demonstrated that higher levels of chlorpyrifos decrease the development and branching of blood vessels (Priyadarshini et al., 2020). Recent findings have raised concerns about the impact of flubendiamide on non-target species (Li et al., 2014; Sarkar et al., 2014, 2017, 2018). This study aims to unravel the mechanisms underlying the irregular vasculature observed in the chorioallantoic membrane of domestic chicks exposed to flubendiamide.

An initial dose range analysis revealed that when early chick embryos were exposed to 500 ppm of flubendiamide (LOEC), their formation of vascular networks in the CAM was hindered. During the course of the development, the treated embryos exhibited symptoms such as bleeding, breakdown of blood vessels and blood clotting.

To address these early findings, morphometric and quantitative analyses were performed to describe the changes in the CAM vasculature. The shortened blood vessels, lower vascular density and fewer vessel junctions indicate a decline in capillary sprouting, which is essential for the formation of blood vessels in the CAM network. However, the rise in lacunarity observed in the embryos exposed to flubendiamide indicated an increase in the number of empty areas not filled by blood vessels. Therefore, it was evident that exposure to flubendiamide caused disorganization of the CAM vasculature by decreasing the formation of capillary sprouts.

The computational docking of flubendiamide to the specific proteins involved in the angiogenesis cascade demonstrated strong binding affinities. The proteins VEGFα (6MXR), CASPASE-3 (4QTX), BMP2 (2GOO), PI3K (1YI3), WNT7A (8TZO) and SHH (3MVX) showed high docking scores. This discovery clearly showed their significant attraction to flubendiamide, indicating its ability to directly interact with and affect these regulators of angiogenesis. The target molecules discovered were subjected to additional screening using transcript and protein level analysis to determine their differential expression pattern during the developmental phase.

VEGFα is an essential signaling molecule that stimulates the growth of new blood vessels, a process known as angiogenesis (Hiratsuka et al., 2005). The connection between KDR (VEGF receptor 2) and Proliferating Cell Nuclear Antigen (PCNA) stimulates the growth of endothelial cells, leading to the formation, sprouting and branching of blood vessels (Hiratsuka et al., 2005; Strzalka & Ziemienowicz, 2011). The reduced expression of VEGFα, KDR and PCNA transcripts, as well as the decreased levels of VEGFα protein in treated embryos on days 2, 3 and 4, suggest impaired proliferation of endothelial cells. Additionally, it has been demonstrated that the SHH signaling pathway influences the cytoskeleton of endothelial cells by regulating the PI3K/AKT pathway (Zavala et al., 2017; Salybekov et al., 2018; Lei et al., 2020). The decreased levels of SHH, AKT and PI3K transcripts, along with reduced expression of PI3K and AKT protein in embryos treated on days 2, 3 and 4, highlight the effectiveness of flubendiamide in targeting these pro-angiogenic factors.

The vascularization of the CAM is maintained through the sprouting of blood vessels, which is then followed by the development of a complete capillary network plexus (Ahmed et al., 2022). The initiation of sprouting is triggered by the activation of WNT7A signaling (Vanhollebeke et al., 2015; Olsen et al., 2017). The decreased amounts of WNT7A transcript on all the chosen experiment days align with the decreased junctions seen in the treated embryos. Moreover, BMP2 and BMP6 preserve the adaptability of endothelial cells while they are sprouting (Benn et al., 2017). These molecules collaborate with SHH and WNT7A to preserve the characteristics of endothelial cells (Olsen et al., 2017). The observed drop in SHH and WNT7A levels thus is directly related to the considerable reduction in BMP2 and BMP6 transcripts on days 2, 3 and 4 in the treated group. These results furthermore suggest the negative impacts of flubendiamide in CAM angiogenesis.

The expression of RHOB and Cl. Caspase-3, two essential components of apoptosis, was also studied in conjunction with the proliferation of endothelial cells. RHOB, which is a member of the Rho GTPase family, is responsible for regulating several cellular processes, including apoptosis (Howe & Addison, 2012). Cleaved Caspase-3, representing an activated form of caspase-3, serves as a diagnostic tool for apoptosis, providing insights into the underlying molecular mechanisms driving cellular death (Brentnall et al., 2013). The expression of RHOB was found to have significantly increased at the transcript level in embryos of day 4 of the experiment. In a similar manner, there was a significant rise in the expression of Cl. Caspase-3 in the treated group's embryos on day 2, day 3 and day 4 and this increase was observed at both the mRNA and protein levels. An additional confirmation of the increased prevalence of Cl. Caspase-3 was obtained using immunolocalization. These findings support the conclusion that inhibited proliferation and increased apoptosis contribute to the disruption of CAM vascularization.

The present investigation on embryonic chick development sought to elucidate the mechanisms by which pesticides such as flubendiamide impede crucial developmental processes and pose health risks to humans. One of the most common outcomes of exposure to flubendiamide is the inhibition of CAM angiogenesis. Flubendiamide significantly disturbed the process of blood vessel formation by targeting multiple signaling pathways. Inhibition of VEGF-KDR signaling disrupted the proliferation of endothelial cells by halting PCNA. Concurrently, flubendiamide upregulated the expression of Cl. Caspase-3 and RHOB, potentially resulting in increased apoptosis levels. Additionally, it suppressed the expression of SHH, BMP2, BMP6 and WNT7A, which hindered blood vessel growth and prevented the development of the capillary network in the CAM, ultimately causing disturbed angiogenesis in the CAM. Further research is necessary to comprehensively understand the intricate molecular mechanisms involved in the effects of flubendiamide on embryonic development.

TABLES

Table 4.1: Comparative analysis of anti-angiogenic property of flubendiamide using CAM angiogenesis.

Group	Percentage Vessel Density	
	Day 3	**Day 4**
Control	39.68 ± 0.47	53.36 ± 0.48
Treated	26.39 ± 0.54***	27.64 ± 0.46***

Data representing the percent vessel density in the control and treated CAM. The values are expressed as Mean ± SEM; n=6. The comparison for statistical significance is done with the control group, ***p≤0.001.

Table 4.2: Molecular Docking study of Flubendiamide PDB IDs VEGFα (6MXR), CASPASE-3 (4QTX), BMP2 (2GOO), PI3K (1YI3), WNT7A (8TZO) and SHH (3MVX) their bonding, amino acid interactions and docking score.

Compound	PDB ID	Bond	Amino Acid Interactions	Docking Score Kcal/mol
Flubendiamide	VEGFα (6MXR)	Conventional Hydrogen Bond Halogen (Fluorine) Carbon Hydrogen Bond Pi-Alkyl	ARG30, GLY68, TYR56, TRP50, GLY31, TRY32	-8.3
	CASPASE- 3 (4QTX)	Conventional Hydrogen Bond Halogen (Fluorine) Carbon Hydrogen Bond Pi-Alkyl Pi-Sigma	ILE187, LYS154, SER150, ARG149, THR152, TYR41	-7.2
	BMP2 (2GOO)	Conventional Hydrogen Bond Halogen (Fluorine) Carbon Hydrogen Bond Pi-Alkyl Alkyl Pi-Anion	ARG16, ASP63, ASP62, ILE64, HIS39, ILE87, VAL107, GLU109	-7.3

	PI3K (1YI3)	Conventional Hydrogen Bond Halogen (Fluorine) Pi-Sulphur	HIS157, GLN150, GLU181, SER101, GLU153	-7.4
	WNT7A (8TZO)	Conventional Hydrogen Bond Halogen (Fluorine) Carbon Hydrogen Bond Pi-Alkyl Pi-Sulphur Pi-Pi Stacked	TRP322, LEU122, ASP125, GLY124, PHE74, LYS43, ASN123	-8.7
	SHH (3MVX)	Conventional Hydrogen Bond Halogen (Fluorine) Pi-Alkyl Alkyl	GLN39, GLY100, GLY101, LYS103, PHE10, LYS9, VAL85, ILE89	-8.2

Table 4.3: Transcript level expression of genes involved in CAM angiogenesis in Flubendiamide treated day 2, day 3 and day 4 embryos.

Gene	**Fold change Day 2**	**Fold change Day 3**	**Fold change Day 4**
SHH	0.993 ± 0.012^{ns}	0.933 ± 0.017^{ns}	$0.790 \pm 0.015^{*}$
VEGFα	$0.403 \pm 0.043^{**}$	0.914 ± 0.08^{ns}	$0.605 \pm 0.020^{**}$
KDR	0.861 ± 0.011^{ns}	0.959 ± 0.06^{ns}	$0.790 \pm 0.015^{*}$
CASPASE-3	$2.982 \pm 0.048^{**}$	$4.993 \pm 0.09^{***}$	$1.833 \pm 0.033^{**}$
WNT7A	0.861 ± 0.011^{ns}	0.688 ± 0.013^{ns}	$0.790 \pm 0.015^{*}$
BMP2	$0.530 \pm 0.013^{*}$	0.953 ± 0.018^{ns}	$0.322 \pm 0.047^{***}$
BMP6	0.861 ± 0.011^{ns}	$0.637 \pm 0.063^{*}$	$0.790 \pm 0.015^{*}$
AKT	$0.657 \pm 0.061^{*}$	$0.432 \pm 0.069^{*}$	0.759 ± 0.024^{ns}
PI3K	$0.431 \pm 0.016^{*}$	0.973 ± 0.022^{ns}	$0.882 \pm 0.041^{*}$
PCNA	$0.071 \pm 0.009^{**}$	$0.555 \pm 0.072^{*}$	1.629 ± 0.027^{ns}
RHOB	0.756 ± 0.021^{ns}	2.114 ± 0.022^{ns}	1.419 ± 0.071^{ns}

Fold changes are expressed as Mean ± SEM. Fold change values for the control embryo is 1.0 for all the genes; n=3 with 30 eggs per group per experiment, ns = not significant, *p≤0.05; **p≤0.01; ***p≤0.001

Table 4.4: Spot densitometry analysis of the western blot bands on day 2, 3 and 4 embryos.

Protein	Band intensity in arbitrary units	
	Control	**Treated**
Day 2		
Vegfα	132.25 ± 1.07	118.63 ± 1.11*
Akt	133.44 ± 1.17	85.24 ± 0.95**
Pi3k	163.68 ± 0.71	134.27 ± 0.50**
Cl. Caspase-3	108.46 ± 0.89	132.50 ± 0.52**
GAPDH	135.88 ± 0.84	127.73 ± 1.03
Day 3		
Vegfα	124.59 ± 0.99	114.83 ± 1.09**
Akt	126.74 ± 0.68	116.91 ± 0.88**
Pi3k	65.22 ± 0.44	47.11 ± 0.78**
Cl. Caspase-3	164.49 ± 0.69	188.76 ± 0.57***
GAPDH	143.27 ± 0.35	142.20 ± 0.39
Day 4		
Vegfα	141.83 ± 0.70	120.44 ± 0.65**
Akt	125.83 ± 0.52	85.53 ± 0.58***
Pi3k	154.98 ± 0.86	105.75 ± 0.76**
Cl. Caspase-3	109.58 ± 1.20	126.54 ± 1.07*
GAPDH	127.51 ± 0.53	130.65 ± 0.54

The values are expressed as Mean ± SEM; n=3 with 30 eggs per group per experiment; *p≤0.05; **p≤0.01; ***p≤0.001

GRAPHICAL SUMMARY